

## UPDATE IN RADIOLOGY

# Vascular compression syndromes: the value of Doppler ultrasonography<sup>☆</sup>



E. Rangel Villalobos<sup>\*</sup>, T. Busquier Cerdán, X. Cortés Sañudo, I. Avilés Vázquez, R. Estellés López, C. Pérez Ramírez

*Departamento de Radiodiagnóstico, Hospital Universitario Virgen Macarena, Sevilla, Spain*

Received 12 November 2019; accepted 2 August 2021

## KEYWORDS

Doppler ultrasound;  
Thoracic outlet  
syndrome;  
Renal nutcracker  
syndrome;  
Median arcuate  
ligament syndrome;  
Popliteal artery

**Abstract** Vascular compression syndromes arise when a vessel in a tight anatomic space is entrapped by another structure, resulting in diverse symptoms for which different imaging tests are used to diagnose. Radiologists need to be familiar with vascular compression syndromes and to be able to identify their most representative findings. This paper aims to review the principal symptoms of vascular compression, describing and illustrating the key findings on Doppler ultrasonography that enable accurate diagnosis and guide further workup, avoiding unnecessary invasive tests and pointing to the appropriate treatment.

© 2021 SERAM. Published by Elsevier España, S.L.U. All rights reserved.

## PALABRAS CLAVE

Ecografía Doppler;  
Síndrome del  
desfiladero torácico;  
Síndrome de  
cascanueces renal;  
Síndrome del  
ligamento arcuato  
medio;  
Arteria poplítea

## Síndromes de compresión vascular. Valor de la ecografía Doppler

**Resumen** Los síndromes de compresión vascular consisten en el atrapamiento de un vaso por otra estructura en un espacio anatómico reducido, lo que provoca sintomatología diversa y para cuyo diagnóstico se emplean diferentes pruebas de imagen. Es importante familiarizarse con este tipo de patología y ser capaces de identificar sus hallazgos más representativos. El objetivo de este artículo es revisar los principales síndromes de compresión vascular, aportando datos clave de hallazgos en la ecografía Doppler que permitan establecer un diagnóstico acertado, evitar otras pruebas más agresivas o seleccionar aquellos pacientes que las requieran y orientar el tratamiento adecuado.

© 2021 SERAM. Publicado por Elsevier España, S.L.U. Todos los derechos reservados.

<sup>☆</sup> Please cite this article as: Rangel Villalobos E, Busquier Cerdán T, Cortés Sañudo X, Avilés Vázquez I, Estellés López R, Pérez Ramírez C. Síndromes de compresión vascular. Valor de la ecografía Doppler. Radiología. 2022;64:17–25.

<sup>\*</sup> Corresponding author.

E-mail address: [eranvilla@yahoo.es](mailto:eranvilla@yahoo.es) (E. Rangel Villalobos).

## Introduction

Vascular compression syndromes consist of entrapment of a vessel by another structure in a limited anatomical space. They usually occur in young people, with various symptoms depending on the structure involved. Their diagnosis requires a combination of clinical signs and imaging findings; the techniques used at present are Doppler ultrasound, computed tomography (CT) angiography and magnetic resonance (MR) angiography. Treatment options will depend on the seriousness of the symptoms and of the associated complications.

This article presents the significant findings in the most common vascular compression syndromes: *thoracic outlet syndrome*, *median arcuate ligament syndrome*, *nutcracker syndrome* and *popliteal artery entrapment syndrome*.

Doppler ultrasound, the imaging method of choice for most of these syndromes, is notable for being a quick, inexpensive, non-invasive and dynamic examination.

A review of the most important general considerations in vascular compression syndromes and their corresponding findings on Doppler ultrasound is presented below.

## Vascular compression syndromes

### Thoracic outlet syndrome

Thoracic outlet syndrome (TOS) is a syndrome caused by compression of the subclavian vessels and/or brachial plexus at the superior thoracic outlet. Depending on the structures affected, it may be: neurological (95%), venous (4%) or arterial (1%).<sup>1</sup>

The superior thoracic outlet is the anatomical segment from the cervical spine to the mediastinum and the upper border of the pectoral muscle. It includes three different anatomical spaces: the interscalene triangle, the costoclavicular space and the retropectoralis minor space. Most vascular compression syndromes occur in the costoclavicular space (Fig. 1).<sup>2</sup> The possible causes are anatomical abnormalities and post-traumatic lesions.

Several tests elicit symptoms and confirm the diagnosis; Allen's test and Adson's test (Fig. 2) are the most commonly used ones<sup>2</sup>:

**Adson's test:** locate the patient's radial pulse and ask them to take a deep breath and turn their head toward the

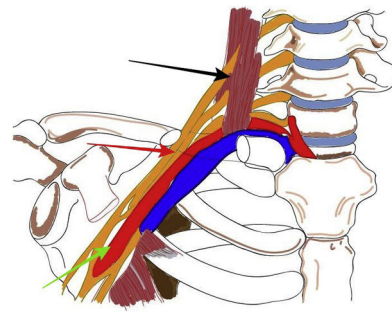


**Figure 1** Anatomy of the superior thoracic outlet. Interscalene (black arrow), costoclavicular (red arrow) and retropectoral (green arrow) spaces.

side being examined. The test is considered positive when the radial pulse is reduced or disappears. It indicates vascular compression by the scalene muscle against the first rib.

**Allen's test:** while palpating the radial pulse, externally rotate and abduct the patient's arm at a 90-degree angle. It is considered positive when the pulse is decreased or abolished. It indicates vascular compression due to the tendon of the pectoralis major muscle.

Signs and symptoms usually appear when the arm is raised and lowered, and vary depending on the point of compression and on the structures affected. Neurological symptoms, secondary to compression of the brachial plexus, are the most common and usually include pain, weakness, numbness and tingling in the affected limb. When compression is venous, signs and symptoms consist of oedema, cyanosis and pain. If compression is arterial, it will manifest as weakness, coldness and pain.<sup>1,2</sup>

### Diagnostic imaging

Doppler ultrasound evaluates indirect signs of stenosis, but does not allow for an accurate assessment of the point of compression or determine the cause.<sup>1</sup> The fundamental advantage of this technique is that it enables a dynamic assessment in a resting position with provocative manoeuvres.<sup>2</sup>

Perform the examination with the patient seated. Place the transducer below the clavicle, in the costoclavicular space. Assess the subclavian artery and vein in a neutral

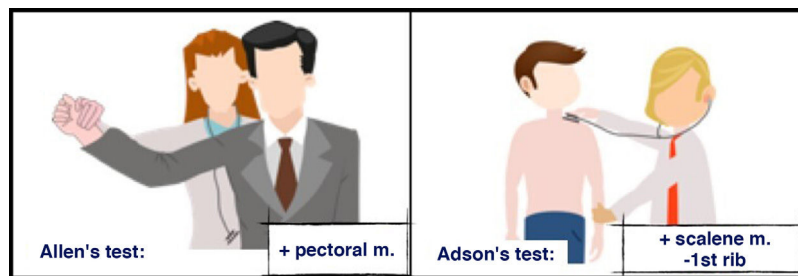


**Figure 2** Allen's test: assesses the radial pulse with the patient's arm at a 90-degree angle, in external rotation and abduction. It is positive when the pulse is abolished or reduced, indicating vascular compression by the tendon of the pectoralis major muscle. Adson's test: assesses the radial pulse in inspiration and rotation of the head towards the side being examined. It is considered positive when the radial pulse is reduced or abolished, indicating vascular compression by the scalene muscle.

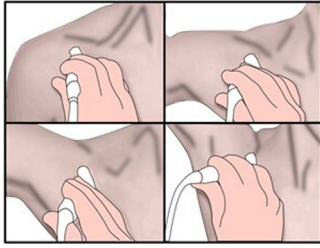


**Figure 3** Modified Adson's manoeuvre: with the patient seated, place the transducer below the clavicle, in the costoclavicular space. Assess the subclavian artery and vein in a neutral position and in progressive abduction/hyperabduction while performing contralateral extension of the neck.

position with a modified Adson's manoeuvre (Fig. 3), consisting of progressive abduction/hyperabduction of the arm and contralateral extension of the neck. Next, assess the radial artery in a neutral position with Allen's and Adson's provocative manoeuvres. In both positions, determine the calibre, flow pattern and peak systolic velocities (PSVs). CT angiography in hyperabduction is usually necessary to gather information on the exact point of compression and the cause.

The most significant Doppler findings are duplication of PSV compared to its value at rest in the subclavian artery and loss of respiratory dynamics in the subclavian vein in 90-degree abduction. Complete cessation of arterial and/or venous blood flow in hyperabduction indicates complete

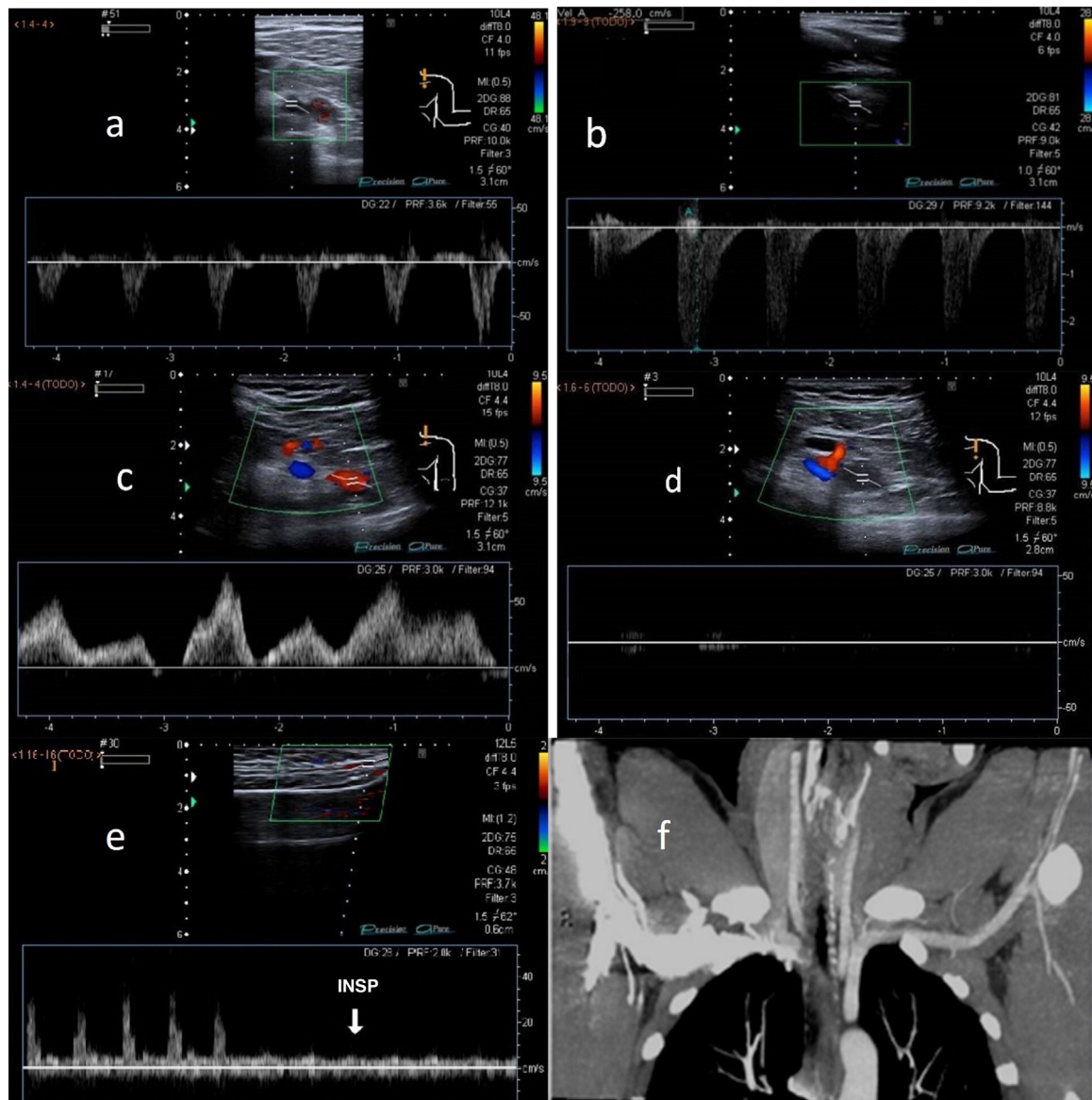


**Figure 4** A) Normal arterial blood flow in a neutral position of the subclavian artery. B) Duplication of PSV in the subclavian artery in 90-degree abduction in thoracic outlet syndrome (TOS). C) Normal venous blood flow in a neutral position of the subclavian vein. D) Loss of respiratory dynamics in the subclavian vein with abduction manoeuvres in TOS. E) Normal radial artery wave in a neutral position and attenuated with Adson's manoeuvre in TOS. F) Contrast-enhanced computed tomography, in a coronal projection, showing left subclavian artery compression in the costoclavicular region.

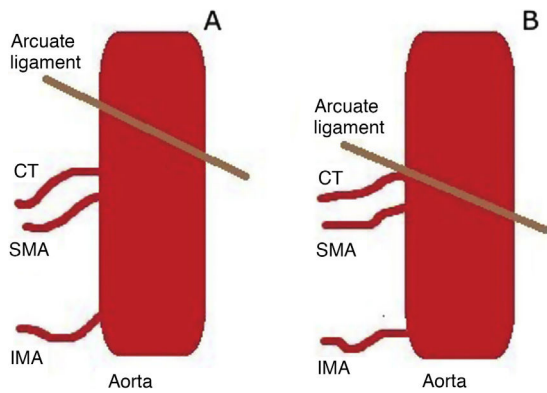


**Figure 5** Figure A shows normal anatomy. Figure B shows how the arcuate ligament is in contact with the outlet of the coeliac trunk. CT: coeliac trunk; IMA: inferior mesenteric artery; SMA: superior mesenteric artery.

occlusion.<sup>2,3</sup> Another finding is attenuation of radial flow with Allen's and Adson's manoeuvres (Fig. 4).

### Median arcuate ligament syndrome

The arcuate ligament is a fibrous structure that connects the two crura of the diaphragm to one another. Its anterior aspect wraps around the aorta at the aortic hiatus. In most cases it is cranial to the coeliac trunk, at the height of the D12-L2 vertebrae, but in some cases the ligament has a low location, in contact with the origin of the coeliac trunk<sup>5</sup> (Fig. 5).

Coeliac trunk compression syndrome is a rare abnormality that predominantly occurs in women 20-40 years of age. This syndrome is clinically characterised by intermittent post-prandial epigastric pain, nausea, vomiting, diarrhoea and weight loss. The abdominal pain may be associated with activities other than eating.<sup>4,6</sup>

The findings reported on physical examination include an epigastric bruit that varies with respiration and is more marked in deep expiration. These symptoms are due to flow compromise caused by the displacement of the ligament.<sup>6</sup>

### Diagnostic imaging

Doppler ultrasound is used to diagnose median arcuate ligament syndrome, revealing a change in the orientation of coeliac trunk in relation to inspiration and expiration (Fig. 6).

For diagnosis, observation of elevated PSVs in maximum expiration exceeding 200 cm/s with a coeliac trunk-to-aorta ratio greater than 3 is indicative of significant blood flow compromise (Fig. 6B and c).

This technique is very commonly used, especially in evaluating blood vessels in children and adolescents.<sup>4</sup> Placing the transducer in B-mode on the axial plane could reveal how the coeliac trunk is compromised and distorted between the abdominal aorta dorsally and the arcuate ligament ventrally.<sup>5,7</sup>

CT angiography is often necessary to assess the degree of stenosis. Superior pressure against the origin of coeliac trunk, causing it to take on a hooked or J-shaped appear-

ance, is characteristic. Another radiological finding is the "hair bun and shawl" sign, which consists of visualisation on a single axial plane of the compromised, distorted coeliac trunk between the abdominal aorta dorsally and the median arcuate ligament ventrally, which practically surrounds the other two. These findings resemble a head (the aorta) with the hair in a bun (the origin of the coeliac trunk), covered by a shawl (the median arcuate ligament). This enables diagnosis in non-targeted examinations and screening of patients to undergo examinations.<sup>8</sup>

### Nutcracker syndrome

This is a syndrome caused by entrapment of the left renal vein (LRV) between the superior mesenteric artery (SMA) and the aorta (anterior nutcracker syndrome), due to a decrease in the angle formed by the two vessels (aortomesenteric angle), with a normal value usually between 38 degrees and 65 degrees (Fig. 7). The LRV sometimes follows a retroaortic or circumaortic path, and may be compressed between the aorta and the spinal column (posterior nutcracker syndrome).<sup>9-11</sup> The two syndromes, anterior and posterior, may coexist due to LRV duplication, though this is not a common finding.<sup>12</sup> In an analogous clinical condition, Wilkie syndrome, the third part of the duodenum is compressed between the SMA and the aorta, resulting in bowel obstruction.<sup>13</sup>

The anatomical configuration can be considered a variant of normal anatomy. Therefore, the term *nutcracker syndrome* should be reserved for patients with characteristic clinical symptoms (LRV hypertension with macroscopic haematuria, left flank pain, orthostatic proteinuria, perireteral varices, gonadal varices and varicocele) associated with demonstrable morphological characteristics.<sup>1,14</sup>

Due to the variability of its symptoms and the lack of a consensus on the criteria for its diagnosis, its exact prevalence is unknown; however, it is thought to be most common in young people, primarily in women in their 20s and 30s. These women may experience pelvic congestion syndrome, which presents with pelvic pain; varices in the genitals, pelvis and thighs; dysmenorrhoea; dyspareunia; and postcoital pain. In men, testicular vein reflux causes a varicocele, left testicular pain and infertility.<sup>1,10,12</sup>

### Diagnostic imaging

Selective LRV venography is considered the most accurate method for diagnosing this nutcracker syndrome. Given that it is an invasive test that is not essential for diagnosis, it is being replaced by other diagnostic imaging techniques: B-mode ultrasound, Doppler ultrasound, CT angiography and MR angiography.<sup>11,12,14</sup>

B-mode ultrasound has been proposed as a method for measuring the aortomesenteric angle, as well as calculating the ratio of the diameter of the dilated part of the LRV to the narrow part thereof and the distance between the aorta and the superior mesenteric artery, respectively. The cut-off points are an angle <25°, ratios >4.5 and a distance <8 mm, respectively. The difference in diameters between the right



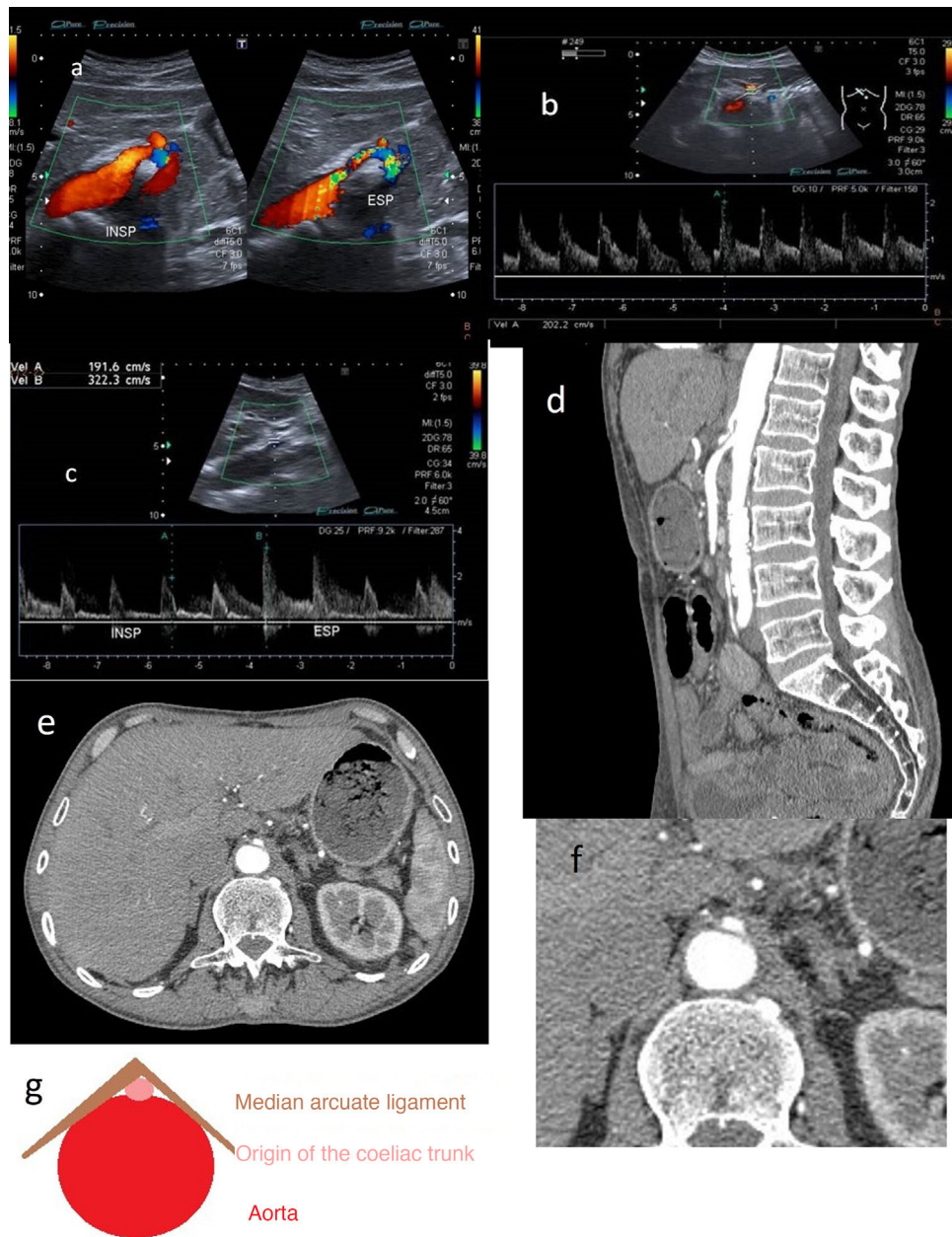


**Figure 6** A) Hook-shaped coeliac trunk with change in orientation in relation to inspiration and expiration. B) Coeliac trunk with elevation of peak systolic velocities  $>200$  cm/s. C) In expiration, the velocity increases from 192 to 322 cm/s. D) CT angiography: (expiration) focal stenosis of the proximal portion of the coeliac trunk (hooked appearance). E and F (detail): CT angiography (arterial phase) showing the “hair bun and shawl” sign. G) “Hair bun and shawl” sign.

and left renal veins has also been used, though it is not a very widely accepted criterion (Fig. 8).

Doppler ultrasound measures the flow velocity of the LRV at the aortomesenteric angle, as well as the diameter and maximum flow velocity in the renal vein before and after it passes through the aortomesenteric angle, with a sensitivity of 78% and a specificity of 100%.

A maximum speed of the renal vein at the angle greater than 100 cm/s is considered abnormal (non-essential crite-

rión). A distal-to-proximal ratio greater than 5 is diagnostic for this syndrome (Fig. 8C).

As this is a harmless technique, it may be useful in screening for orthostatic proteinuria. In our setting, other diagnostic tests usually do not need to be performed in most paediatric patients. CT angiography or MT angiography may be required in adults depending on the therapeutic approach.<sup>15</sup>

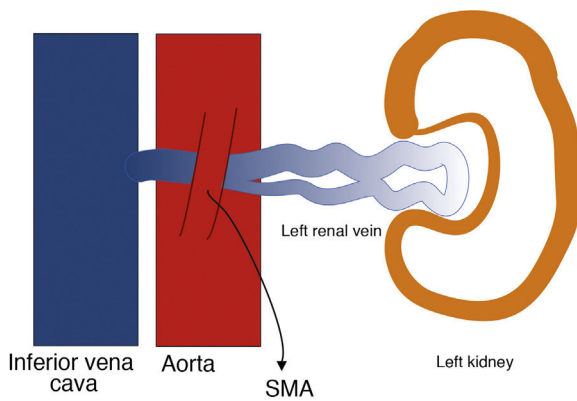


**Figure 7** Anatomy of nutcracker syndrome. SMA: superior mesenteric artery.

## Popliteal artery entrapment syndrome

Popliteal artery entrapment syndrome (PAES) is a vascular compression syndrome that affects the popliteal artery (PA) at the proximal insertion of both heads of the gastrocnemius muscle. Normally, the PA runs between the two heads of that muscle, along with the popliteal vein and the popliteal nerve.<sup>16</sup> This rare syndrome most often affects young men and in most cases is bilateral. It may be explained by an abnormality in embryogenesis during the formation of the PA and in the migration of the gastrocnemius muscle.<sup>17</sup>

The signs and symptoms are usually exercise-induced claudication and pain. Lack of treatment leads to artery damage, thrombosis and ischaemia in the leg.<sup>18</sup> It is classified according to the classification that was published by Love and Whelan in 1965 and modified by Rich in 1979, based on anatomical variants<sup>16,19</sup>:

- Type I: the PA follows an aberrant path medial to the head of the gastrocnemius muscle (HGM).
- Type II: the HGM shows an abnormal femoral insertion that is more lateral than usual, leaving the PA on its medial side.
- Type III: an accessory muscle band of the HGM inserts more laterally and separately, surrounding the PA.
- Type IV: the PA is located deep in the popliteal fossa and is found to be compressed by the popliteal muscle or fibrous bands.
- Type V: any form of entrapment that includes the popliteal vein in addition to the PA.
- Type VI: there are no abnormalities along the path of the artery or in the insertions or morphology of the gastrocnemius muscle, but these compress the vascular bundle.

## Diagnostic imaging

Doppler ultrasound is used as a screening method, as it is non-invasive and does not emit radiation. Examination of the PA starts above the knee joint until it bifurcates bilaterally. The examination is performed with the patient in prone decubitus, with the leg extended and in a neutral position to determine the changes in the vessel intima and the presence of stenosis or aneurysms, as well as the veloc-

ity and shape of the spectral curve.<sup>16,18</sup> The second part of the examination consists of stress manoeuvres, in which the ankle is placed in dorsiflexion and plantar flexion for up to 30 seconds; the radiologist may aid in maintaining the posture by applying pressure (Fig. 9A). Next, the patient will stand on tiptoe.<sup>15,16</sup> At this point, blood flow all along the path of the PA will be evaluated and the presence or absence of blood flow and the decrease in the systolic peak will be determined using stress manoeuvres (Fig. 9B). The dorsalis pedis artery and the posterior tibial artery can also be assessed.<sup>17,19</sup>

PA stenosis can be quantified by measuring the PSV ratio in the lesion: the PSV is measured at the stenosis and compared to the contralateral healthy artery, creating a specific ratio for each patient. Radonic V. et al. (2000) found that a ratio greater than 2 would indicate significant stenosis.

Turbulent flow with aliasing is necessary for detecting haemodynamically significant stenosis. Vessel obstruction is considered to be present if blood flow is detected by neither colour nor pulsed-wave Doppler ultrasound<sup>18</sup> (Fig. 10). For proper visualisation of anatomical variants, the examination can be supplemented with MR angiography.

## Conclusions

Vascular compression syndromes are uncommon and difficult to diagnose. The characteristic symptoms are due to intermittent compression of the neurovascular bundle as it passes through different anatomical outlets. Doppler ultrasound is indicated in the first-level diagnosis of vascular compression syndromes as it evaluates the presence, type and grade of haemodynamic compromise at different vascular levels, and will confirm or be confirmed by other diagnostic tests. The fundamental advantage of this technique is that it enables non-invasive, dynamic patient assessment in real-time with provocative manoeuvres. The radiologist should be familiar with the protocol for evaluation and interpretation of the results, which can influence the diagnostic and therapeutic management of patients, as well as post-treatment follow-up. Extending the radiological study with tests such as MR angiography and CT angiography is especially important in TOS and SAP, as they enable suitable assessment of the relationship of vascular structures to anatomy.

## Authorship

- 1 Responsible for study integrity: ERV, TBC, XCS, IAV, REL and CPR
- 2 Study concept: ERV, TBC, XCS, IAV, REL and CPR
- 3 Study design: ERV, TBC, XCS, IAV, REL and CPR
- 4 Data collection: ERV, TBC, XCS, IAV, REL and CPR
- 5 Data analysis and interpretation: ERV, TBC, XCS, IAV, REL and CPR
- 6 Statistical processing: ERV, TBC, XCS, IAV, REL and CPR
- 7 Literature search: ERV, TBC, XCS, IAV, REL and CPR
- 8 Drafting of the article: ERV, TBC, XCS, IAV, REL and CPR
- 9 Critical review of the manuscript with intellectually significant contributions: ERV, TBC, XCS, IAV, REL and CPR
- 10 Approval of the final version: ERV, TBC, XCS, IAV, REL and CPR

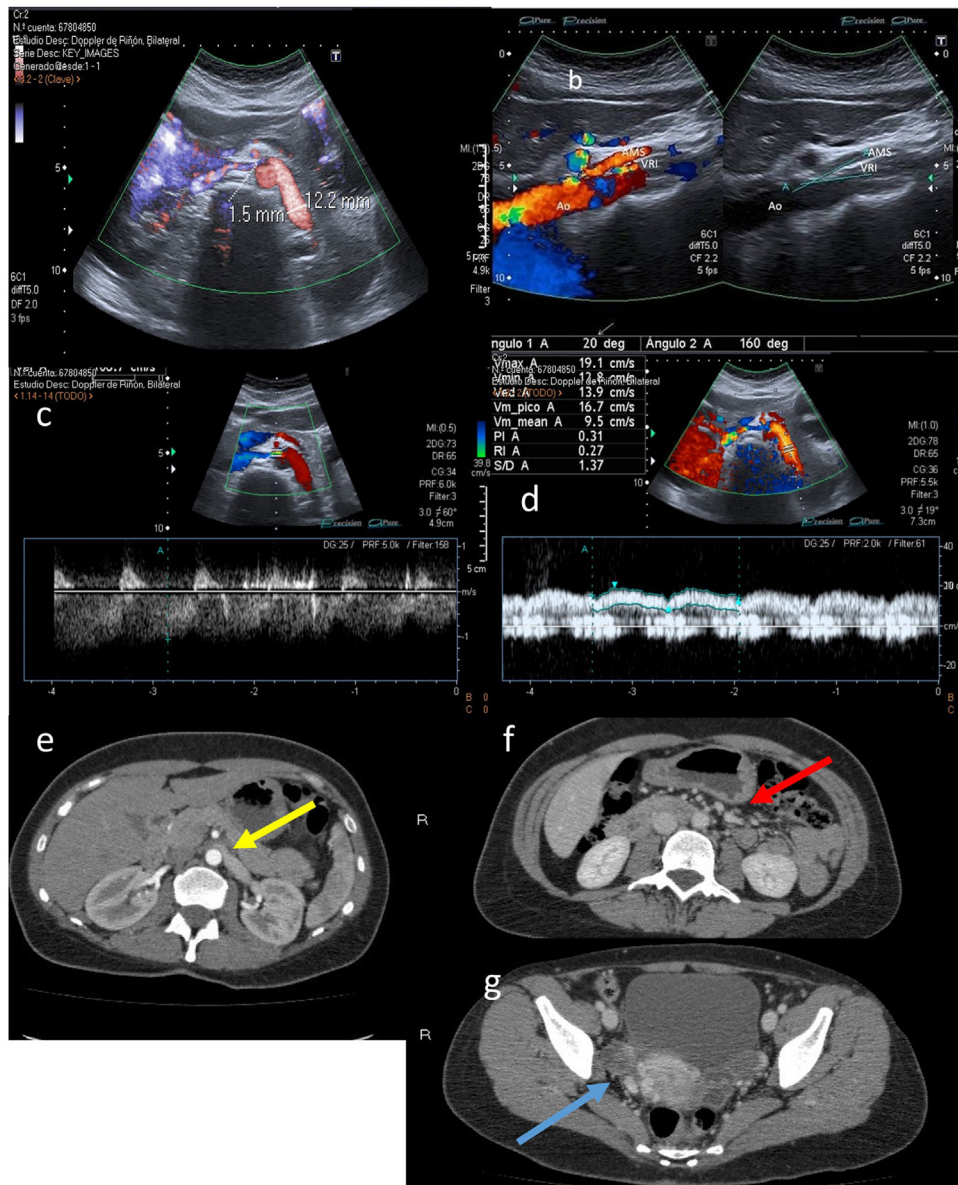


**Figure 8** A) Calibre of the left renal vein (LRV) in the hilar region (before the angle): 12.2 mm. LRV calibre at the angle itself between the aorta (Ao) and the superior mesenteric artery (SMA): 1.5 mm. B) Decreased aortomesenteric angle at the LRV (20°). C) Increased LRV velocity at the aortomesenteric angle (106 cm/s). D) Normal LRV velocity prior to the angle (19 cm/s). E-G) Axial projections from contrast-enhanced computed tomography of abdomen in arterial phase (E) and portal phase (F and G). Image E shows a reduction in the calibre of the LRV as it passes through the aortomesenteric angle (yellow arrow). Image F shows slightly dilated gonadal veins (red arrow). Right parauterine varices are visible in Image G (blue arrow).



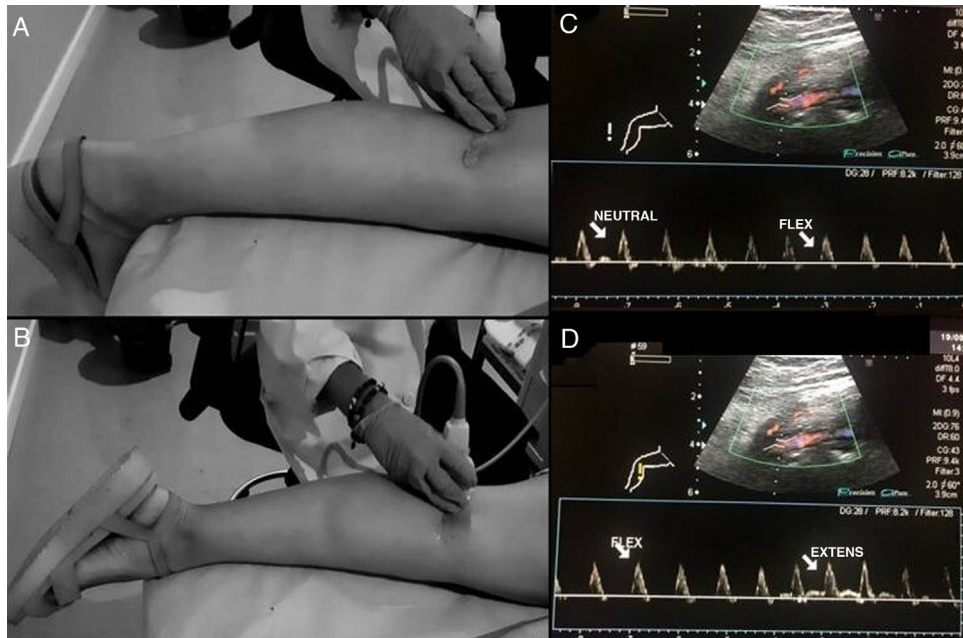


**Figure 9** Stress manoeuvres for assessing popliteal artery entrapment syndrome. Patient in prone decubitus, with the leg extended and the ankle in dorsiflexion (A) and plantar extension (B) for 30 seconds. The radiologist can help to maintain the posture by applying pressure. The presence or absence of or changes in blood flow will be evaluated all along the path of the popliteal artery with changes in position. C and D show normal findings on spectral Doppler ultrasound with flexion and extension stress manoeuvres.

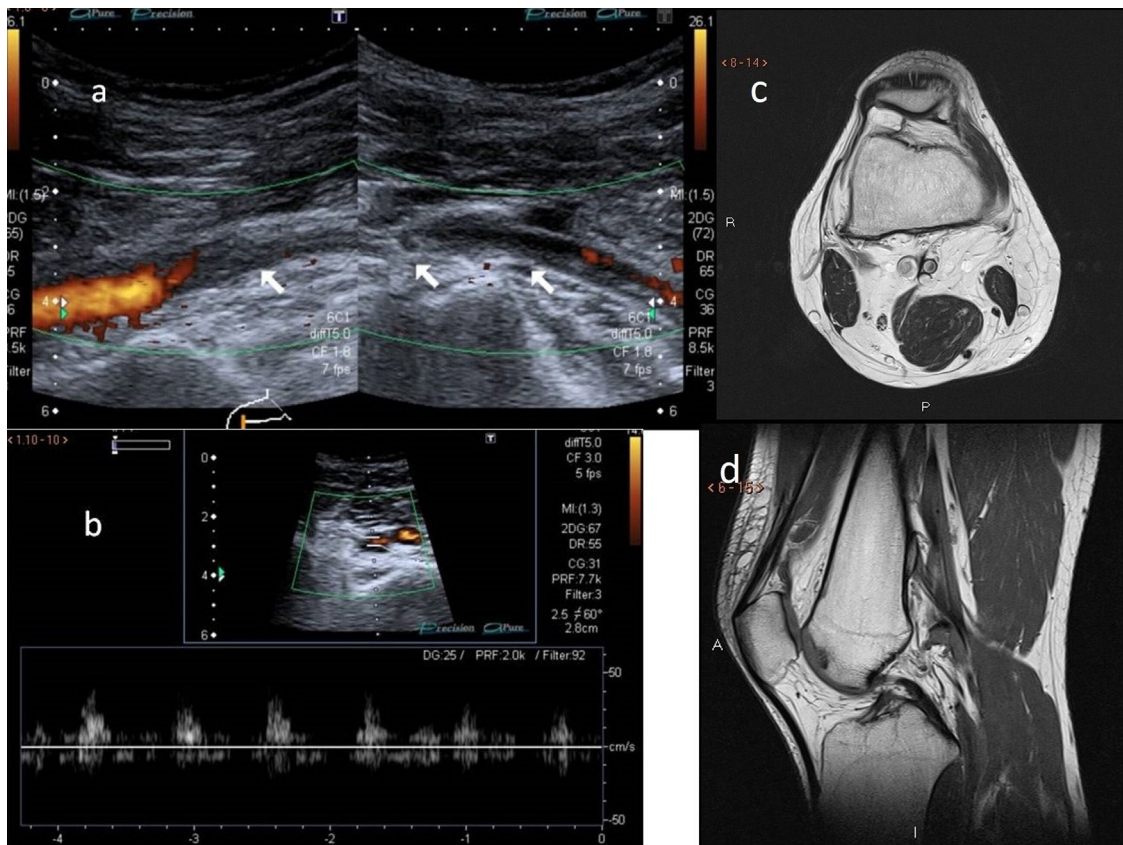


**Figure 10** A and B) Doppler ultrasound. Subocclusion of the popliteal artery with very weak blood flow in a young patient with popliteal artery entrapment syndrome and signs and symptoms of intermittent claudication. C and D) Non-contrast-enhanced magnetic resonance imaging, axial and sagittal projections, respectively. Abnormal insertion of the medial gastrocnemius muscle, the tendon of which ascends more than normal, passing between the popliteal artery and vein and inserting in the posterior cortex of the femoral metaphysis, where a benign bony outgrowth has formed. Modified Love and Whelan II classification.



## Funding

There was no funding for the preparation of this article.

## References

1. Jones M, Prabhakar A, Viswanath O, Urits I, Green J, Kendrick J, et al. Thoracic Outlet Syndrome: A Comprehensive Review of Pathophysiology, Diagnosis, and Treatment. *Pain Ther.* 2019;8:5–18, <http://dx.doi.org/10.1007/s40122-019-0124-2>.
2. Demondion X, Herbinet P, Van Sint Jan S, Boutry N, Chantelot C, Cotten A. Imaging assessment of thoracic outlet syndrome. *Radiographics.* 2006;26:1735–50, <http://dx.doi.org/10.1148/rg.266055079>.
3. Wadhvani R, Chaubal N, Sukthankar R, Shroff M, Agarwala S. Color Doppler and duplex sonography in 5 patients with thoracic outlet syndrome. *J Ultrasound Med.* 2001;20:795–801, <http://dx.doi.org/10.7863/jum.2001.20.7.795>.
4. Schiappacasse G, Maldonado I, Varela C, Muller K, Ortiz J. Síndrome del ligamento arcuato medio. *Rev Chil Radiol.* 2014;20:149–55.
5. Wolfman D, Bluth EI, Sossaman J. Median arcuate ligament syndrome. *J Ultrasound Med.* 2003;22:1377–80, <http://dx.doi.org/10.7863/jum.2003.22.12.1377>.
6. Horton KM, Talamini MA, Fishman EK. Median arcuate ligament syndrome: evaluation with CT angiography. *Radiographics.* 2005;25:1177–82, <http://dx.doi.org/10.1148/rg.255055001>.
7. Scholbach T. Celiac artery compression syndrome in children, adolescents, and young adults: clinical and color duplex sonographic features in a series of 59 cases. *J Ultrasound Med.* 2006;25:299–305, <http://dx.doi.org/10.7863/jum.2006.25.3.299>.
8. Soliva Martínez D, Belda González I, Fernández Iglesias P, Martínez Yunta J. Signo del moño y la mantilla en el síndrome del ligamento arcuato mediano del diafragma. *Rev Argent Radiol.* 2015;79:55–7, <http://dx.doi.org/10.1016/j.rard.2014.12.002>.
9. Weerakkody Y, D'Souza D. Nutcracker syndrome | Radiology Reference Article | Radiopaedia.org [Internet]. <https://radiopaedia.org/articles/nutcracker-syndrome/>; 2019. [accessed el 25 de octubre de 2019].
10. Lamba R, Tanner D, Sekhon S, McGahan J, Corwin M, Lall C. Multidetector CT of Vascular Compression Syndromes in the Abdomen and Pelvis. *Radiographics.* 2014;34:93–115, <http://dx.doi.org/10.1148/rg.341125010>.
11. Taktak A, Hakan Demirkan T, Acar B, Gür G, Köksoy A, Uncu N, et al. Correlación clínico-radiológica del síndrome del cascanueces: Experiencia en un solo centro. *Arch Argent Pediatr.* 2017;115:165–8, <http://dx.doi.org/10.5546/aap.2017.165>.
12. Kim S, Cho S, Kim H, Chung J, Park J, Han M. Nutcracker syndrome: diagnosis with Doppler US. *Radiology.* 1996;198:93–7, <http://dx.doi.org/10.1148/radiology.198.1.8539413>.
13. Suárez-Gutiérrez R, Jiménez-Urueta PS, Castañeda Ortiz RA, Sánchez-Michaca VJ, García-Galavís JL. Megagastria y megaduodeno asociado con síndrome de arteria mesentérica superior y síndrome de cascanueces. *Rev Esp Med Quir.* 2011;16:51–5.
14. Kurklinsky A, Rooke T. Nutcracker Phenomenon and Nutcracker Syndrome. *Mayo Clinic Proceed.* 2010;85:552–9, <http://dx.doi.org/10.4065/mcp.2009.0586>.
15. Fong JK, Poh AC, Tan AG, Taneja R. Imaging findings and clinical features of abdominal vascular compression syndromes. *AJR Am J Roentgenol.* 2014;203:29–36, <http://dx.doi.org/10.2214/AJR.13.11598>.
16. Jarraya M, Simmons S, Farber A, Teytelboym O, Nagara N, Guermazi A. Uncommon Diseases of The Popliteal Artery: A Pictorial Review. *Insights Imaging.* 2016;7:679–88, <http://dx.doi.org/10.1007/s13244-016-0513-6>.
17. Williams C, Kennedy D, Bastian-Jordan M, Hislop M, Cramp B, Dhupelia S. A new diagnostic approach to popliteal artery entrapment syndrome. *J Med Radiat Sci.* 2015;62(Sep):226–9, <http://dx.doi.org/10.1002/jmrs.121>.
18. Radonić V, Koplić S, Giunio L, Božić I, Masković J, Buća A. Popliteal artery entrapment syndrome: diagnosis and management, with report of three cases. *Tex Heart Inst J.* 2000;27:3–13.
19. Carneiro Júnior FCF, Carrijo ENDA, Araújo ST, Nakano LCU, de Amorim JE, Cacione DG. Popliteal Artery Entrapment Syndrome: A Case Report and Review of the Literature. *Am J Case Rep.* 2018;19:29–34, <http://dx.doi.org/10.12659/ajcr.905170>.